

SUPPLEMENTARY MATERIAL:

**Random mutagenesis of a hyperthermophilic archaeon identified
tRNA modifications associated with cellular hyperthermotolerance**

Izumi Orita¹⁾, Ryohei Futatsuishi¹⁾, Kyoko Adachi¹⁾, Takayuki Ohira²⁾, Akira Kaneko¹⁾, Keiichi Minowa²⁾, Miho Suzuki¹⁾, Takeshi Tamura¹⁾, Satoshi Nakamura¹⁾, Tadayuki Imanaka³⁾, Tsutomu Suzuki²⁾, and Toshiaki Fukui¹⁾*

School of Life Science and Technology, Tokyo Institute of Technology, Yokohama, Japan¹⁾,
Department of Chemistry and Biotechnology, Graduate School of Engineering, University of Tokyo,
Tokyo, Japan²⁾, The Research Organization of Science & Technology, Ritsumeikan University,
Kusatsu, Japan³⁾.

Content:

Supplementary Results

Table S1, S2, S3, S4

Figure S1, S2, S3, S4, S5, S6, S7, S8, S9

Supplementary Results

Isolation of 6-methylpurine-resistant mutant for validation of the random mutant library of *T. kodakarensis*

6-Methylpurine (6MP) is known to be toxic for hypoxanthine/guanine phosphoribosyltransferase-positive cells, and TK0664 corresponds to this enzyme in *T. kodakarensis* (1). Three 6MP-resistant mutants could be obtained from the mutant library on 6MP-containing plate medium and showed normal growth on ASW-YT-S⁰ medium containing 0.5 mM 6MP at 85°C (Fig. S1 (B)). As expected, sequencing analysis of the rescued plasmids clarified that all the three mutants had transposon insertion within *tk0664* at which direct repeat region was 139-147 bp (Fig. S1 (C)).

Disruption of predicted restriction endonuclease gene.

The whole genome analysis of *T. kodakarensis* identified 9 genes encoding probable restriction endonucleases. Among them, *tk2239* was disrupted in the Δ *pdaD* strain aiming at improving transformation efficiency, because TK2239 shared 28% identity with a type II restriction endonuclease *PhoI* derived from the closely related hyperthermophile *Pyrococcus horikoshii*.

A DNA fragment of *tk2239* together with the 1-kbp flanking regions was amplified with gDNA of *T. kodakarensis* as a template and a primer set of *tk2239_up/tk2239_down*. The amplified fragment was inserted into pUD3 harboring *pyrF* marker (2) at the *HincII* site. Inverse PCR with a primer pair *tk2239_Inv1/tk2239_Inv2* was then carried out to amplify the flanking regions along with the plasmid backbone, thereby removing the coding region. The amplified fragment was self-ligated after 5'-phosphorylation, and the resulting plasmid was designed as pUD3- Δ 2239. *T. kodakarensis* strains Δ *pdaD* (3) and KU216 (4) were transformed with pUD3- Δ 2239 to obtain strains of Δ 2239 (Δ *pdaD* Δ *pyrF* Δ *tk2239*) and KD2239 (Δ *pyrF* Δ *tk2239*), respectively. Selection of uracil-prototrophic transformants and 5-fluoroorotic acid (5-FOA)-resistant uracil-autotrophic transformants formed by pop-in and pop-out recombination, respectively, were performed according to the procedure described previously (5).

Upon transformation with the transposon-inserted library DNA, the disruptant Δ 2239 showed maximum transformation efficiency of 6×10^3 CFU/ μ g DNA, that was higher than 3×10^3 CFU/ μ g DNA of the parent strain. Further mutagenesis experiments were thus carried out by using Δ 2239 as a host strain. The strain KD2239 was used as a control strain in growth measurement of the isolated mutant strains.

REFERENCES

1. Hileman, T.H. and Santangelo, T.J. (2012) Genetics Techniques for *Thermococcus kodakarensis*. *Front Microbiol*, **3**, 195.
2. Kobori, H., Ogino, M., Orita, I., Nakamura, S., Imanaka, T. and Fukui, T. (2010) Characterization of NADH oxidase/NADPH polysulfide oxidoreductase and its unexpected participation in oxygen sensitivity in an anaerobic hyperthermophilic archaeon. *J Bacteriol*, **192**, 5192-5202.
3. Fukuda, W., Morimoto, N., Imanaka, T. and Fujiwara, S. (2008) Agmatine is essential for the cell growth of *Thermococcus kodakaraensis*. *FEMS Microbiol Lett*, **287**, 113-120.
4. Sato, T., Fukui, T., Atomi, H. and Imanaka, T. (2003) Targeted gene disruption by homologous recombination in the hyperthermophilic archaeon *Thermococcus kodakaraensis* KOD1. *J Bacteriol*, **185**, 210-220.
5. Sato, T., Fukui, T., Atomi, H. and Imanaka, T. (2005) Improved and versatile transformation system allowing multiple genetic manipulations of the hyperthermophilic archaeon *Thermococcus kodakaraensis*. *Appl Environ Microbiol*, **71**, 3889-3899.
6. Atomi, H., Fukui, T., Kanai, T., Morikawa, M. and Imanaka, T. (2004) Description of *Thermococcus kodakaraensis* sp. nov., a well studied hyperthermophilic archaeon previously reported as *Pyrococcus* sp. KOD1. *Archaea*, **1**, 263-267.
7. Fukuda, W., Morimoto, N., Imanaka, T. and Fujiwara, S. (2008) Agmatine is essential for the cell growth of *Thermococcus kodakaraensis*. *FEMS Microbiol Lett*, **287**, 113-120.
8. Santangelo, T.J., Cubonova, L. and Reeve, J.N. (2008) Shuttle vector expression in *Thermococcus kodakaraensis*: contributions of cis elements to protein synthesis in a hyperthermophilic archaeon. *Appl Environ Microbiol*, **74**, 3099-3104.

Table S1. Strains and plasmids used in this study

Strains	Genotypes	Source or reference
<i>Escherichia coli</i>		
DH5 α	ϕ 80 <i>lacZ</i> Δ M15 <i>recA1 endA1 gyrA96 thi-1 hsdR17</i> (r_{k^-} m_k^+) <i>supE44 relA1 deoR</i> Δ (<i>lacZYA-argF</i>) U169 <i>phoA</i>	
HST08	F ⁻ ϕ 80 <i>lacZ</i> Δ M15 <i>recA1 endA1 supE44 thi-1 relA1</i> Δ (<i>lacZYA-argF</i>) U169 Δ (<i>mrr-hsdRMS-mcrBC</i>) <i>gyrA96 phoA</i> Δ <i>mcrA</i> λ^-	Takara Bio
EC100D <i>pir-116</i>	F ⁻ <i>mcrA recA1 endA1</i> Δ (<i>mrr-hsdRMS-mcrBC</i>) ϕ 80 <i>lacZ</i> Δ M15 Δ <i>lacX74 araD139</i> Δ (<i>ara, leu</i>)7697 <i>galU galK</i> λ^- <i>rpsL</i> (<i>Str^R</i>) <i>nupG pir-116</i> (DHFR)	Epicentre
<i>Thermococcus kodakarensis</i>		
KOD1	Wild type	(6)
KU216	Δ <i>pyrF</i> (uracil auxotroph)	(4)
Δ <i>pdaD</i>	Δ <i>pdaD</i> Δ <i>pyrF</i> (agmatine and uracil auxotroph)	(7)
Δ 2239	Δ <i>pdaD</i> derivative, Δ <i>tk2239</i>	This study
KD2239	KU216 derivative, Δ <i>tk2239</i>	This study
Plasmids		
pUC118	Cloning vector, Amp ^r	Takara Bio
pUD3	pUC118 derivative, <i>pyrF</i> marker cassette	(2)
pUD3- Δ <i>tk2239</i>	pUD3 derivative, <i>tk2239 del</i> *	This study
pMOD3	ColE1 ori, Amp ^r , R6K γ ori, mosaic end sequences, MCS	Epicentre
pMOD3- <i>pdaD</i> -Gm	pMOD3 derivative, <i>pdaD_{Tk}</i> , Gm ^r	This study
pLC71	<i>E. coli-T. kodakarensis</i> shuttle vector, Amp ^r , Km ^r , <i>trpE_{Tk}</i> , <i>hmgP_f</i>	(8)
pLCS	pLC71 derivative, Δ <i>trpE_{Tk}</i> ::MCS (NdeI-StuI-SpeI-NheI-SphI)	This study

* Indicates an insert used for targeted gene deletion.

Table S2. Primer sequences used in this study.

Primer	Sequence (5'→3')	Site and others
tk2239_up	CTTGCTCCCCGCTCATCTTGCCCTTC	
tk2239_down	GAAGCTCTTCATAGCAAGGCTGTGCGAG	
tk2239_Inv1	TTCGATCACCGTTTTATTTTTCTGTGCG	
tk2239_Inv2	GCAAGGTATATAACCCTCCTCACGC	
tk0149-f	GTTCTAGAGGCCTTCCTTGACCTTGTA	
tk0149-r	AATCTAGATCAGTAGGGGAACATGACGACG	
tk0149-N	ATGAGCTGGACAACCCCAAAG	
GAT-f2	TGCCGGGTGACGCACACCGT	
GAT-r2-Age	GCAT <u>ACCGGT</u> ACAAGGACAATTAACAGTT	AgeI
pMOD3-MCS-Fw	ATTCAGGCTGCGCAACTGT	
pMOD3-MCS-Rv	GTCAGTGAGCGAGGAAGCGGAAG	
pMOD3-SqFp	GCCAACGACTACGCACTAGCCAAC	
pMOD3-SqRp	GAGCCAATATGCGGAGAACACCCGAGAA	
pLC71-inv1DKanr	<u>TACTAGTGCTAGCGCATGCCTTCTATCGCCTTCTTGACG</u> AGTTCTTCTG	SpeI-NheI-SphI
pLC71-inv2	GGCCT <u>CATATGCATCACCTTTTTAA</u> CGGCCCTCTC	NdeI
mEzTN5SqFp	AAACATGAGAGCTTAGTACGTAATC	
mEzTN5SqRp	TTTTTATTGTTAACTGTTAATTGTCCT	
EzTN5SqFp	GGTTGAACTGCCAACGACTACGCACTA	
EzTN5SqRp	CGAATTCGAGCCAATATGCGGAGAACACCCGAGAA	
tk0754-Fw-NdeI	GGAATTCC <u>CATATG</u> ACCGTCAAGGTCCGCTTT	NdeI (FFH02)
tk0754-Rv-SphI	ACAT <u>GCATGCT</u> CAGGTGAGAAGCCTCTTGTA	SphI (FFH02)
tk0760_NdeN	GGAATTCC <u>CATATG</u> GTTCGATTTCAGGTTGAGGTC	NdeI (FFH18)
tk0760_XbaC	GCT <u>CTAGACT</u> ACTTCTCGACTCCCCTCCTAAC	XbaI (FFH18)
tk0981_NdeN	GGAATTCC <u>CATATG</u> CTCTACGTGGAGATACTCGGAAAC	NdeI (FFH35)
tk0981_SpeC	CTGTTATAGTT <u>ACTAGT</u> TCAATTCTCAAACACATAGAAGT ACC	SpeI (FFH35)
tk1198-Fw-NdeI	GGAATTCC <u>CATATG</u> AGGGTGATAATGGCCGA	NdeI (FFH05)
tk1198-Rv-SphI	ACAT <u>GCATGCT</u> CAAAGCACGTTCCAGGTA	SphI (FFH05)
Tk1328_NdeN	GGAATTCC <u>CATATG</u> ATATCAGTCGGAGATAGAGTTCTTC TC	NdeI (FFH20)
Tk1328_XbaC	GCT <u>CTAGAGT</u> CACAGCTTCCTGAGGAAGGTTATG	XbaI (FFH20)
tk0672-Fw-NdeI	GGAATTCC <u>CATATG</u> AGGTTCTACATCTGCAGGGAA	NdeI (FFH15)
tk0672-Rv-SphI	ACAT <u>GCATGCT</u> CAGCACTTCCCGTTCGC	SphI (FFH15)
tk1803-Fw-NdeI	GGATTCC <u>CATATG</u> GGATTTGGTAGGTACGTGCTGAT	NdeI (FFH12)
tk1803-Rv-SpeI	GG <u>ACTAGT</u> TCACACATTCTGGGATGCACCAACC	SpeI (FFH12)
tk0647-Fw-NdeI	GGAATTCC <u>CATATG</u> AACATCCAGAATGCTG	NdeI (FFH27)
tk0647-Rv-SpeI	GG <u>ACTAGT</u> TTAATCAACTTTGAAACACAGAACA	SpeI (FFH27)
tk1402-Fw-NdeI	GGAATTCC <u>CATATG</u> AAAAAATTGCTGGTAATAA	NdeI (FFH08)
tk1402-Rv-SphI	ACAT <u>GCATGCT</u> CAACGTTTCGTGGTTGGGAGA	SphI (FFH08)
tk2145-Fw-NdeI	GGAATTCC <u>CATATG</u> GCTGAAAGCATTGGCG	NdeI (FFH22)
tk2145-Rv-SpeI	GG <u>ACTAGT</u> CACTCCTTGTTACGCCC	SpeI (FFH22)

Table S3. Transposon insertion sites in *T. kodakarensis* partially thermosensitive mutants isolated by random mutagenesis.

Predicted function	Transposon insertion site	Annotation	Mutant strain (Direct repeat region [bp no.])
metabolism	<i>tk0260</i>	aromatic aminotransferase	FFH09 (308-316)
	<i>tk1405</i>	phosphoenolpyruvate carboxykinase	FFH13 (849-857)
	<i>tk1406</i>	maltodextrin phosphorylase	FFH19 (863-871 and 430-bp deletion)
	<i>tk0262</i>	chorismate synthase	FFH37 (691-699)
	<i>tk0245</i>	imidazoleglycerol-phosphate dehydratase HisB	FFH38 (311-319)
cellular process	<i>tk0635</i>	chemotaxis histidine kinase, frame shift	FFH01 (134-142)
	<i>tk1179</i>	adenylate cyclase, class 2	FFH28 (101-109)
	<i>tk1361</i>	MCM2/3/5 family DNA replication licensing factor	FFH29 (420-428)
	<i>tk0701</i>	ATPase (MinD superfamily P-loop ATPase containing an inserted ferredoxin domain)	FFH31 (470-478)
transport	<i>tk0658</i>	simple sugar transport system ATP-binding protein	FFH06 (1076-1084)
	<i>tk0707</i>	ABC-type iron(III)-siderophore transport system permease	FFH10 (not determined) ¹⁾
	<i>tk1771</i>	ABC-type maltodextrin transport system maltodextrin-binding periplasmic protein	FFH23 (1259-1267)
degradation	<i>tk0699</i>	zinc-dependent protease	FFH26 (289-297)
	<i>tk1169</i>	exosome complex RNA-binding protein Csl4	FFH34 (246-254)
	<i>tk2252</i>	proteasome-activating nucleotidase	FFH03 (76-84) FFH04 (547-555)
mobile genetic element	<i>tk0575</i>	integrase, <i>N</i> -fragment	FFH39 (25-33)
unknown	<i>tk0437</i>	hypothetical protein	FFH07 (1210-1218)
	<i>tk2157</i>	hypothetical protein	FFH14 (4-12)
	<i>tk2174</i>	hypothetical protein	FFH30 (127-135)

1) Sequencing of the junction regions was unsuccessful.

Table S4A. List of predicted RNA fragments with G⁺15 (RNase T₁-digestion)

No.	Sequence of RNA fragments	Molecular mass	<i>m/z</i> (-2)	Mass spectrum	CID	Possible tRNAs	# of tRNAs
1	UCUAG ⁺ ACUGp	2935.40	1466.69	Observed	Not assigned	Val(CAC), Val(GAC)	2
2	CCUAG ⁺ CCAGp	2933.43	1465.71	Observed	Assigned	Arg(CCT)	1
3	CCUAG ⁺ UCUGp/ UCUAG+CCUGp/ CUUAG+CCUGp	2911.38	1454.68	Observed	Not assigned	Arg(CCG), Arg(GCG), Arg(TCG), Gly(CCC), Gly(GCC), Gly(TCC), Lys(CTT), eMet(CAT)	8
4	CUCAG ⁺ CCUGp/ CCUAG+CCUGp/ CCUAG+CUCGp	2910.40	1454.19	Observed	Not assigned	Ala(CGC), Ala(GGC), Ala(TGC), Ile(GAT), Ile(CAT), Lys(TTT), Phe(GAA), Ser(CGA), Ser(GCT), Ser(GGA), Ser(TGA), Thr(TGT), Tyr(GTA), Thr(GGT), Thr(CGT)	15
5	UCUAG ⁺ AUGp	2630.35	1314.17	Observed	Assigned	Val(TAC)	1
6	CCUAG ⁺ CAGp	2628.39	1313.19	Observed	Assigned	Arg(TCT)	1
7	CUUAG ⁺ UUGp	2607.33	1302.66	Observed	Assigned	Asn(GTT)	1
8	CCUAG ⁺ AGp	2323.34	1160.66	Observed	Not assigned	Cys(GCA)	1
9	CAG ⁺ CUAGp	2323.34	1160.66	Observed	Assigned	iMet(CAT)	1
10	UAG ⁺ CUUGp	2301.30	1149.64	Observed	Assigned	Pro(CGG), Pro(GGG), Pro(TGG)	3
11	UAG ⁺ CCUGp	2300.32	1149.15	Observed	Assigned	His(GTG), Trp(CCA)	2
12	UAG ⁺ CCCGp	2299.33	1148.66	Observed	Assigned	Asp(GCT), Glu(CTC), Glu(TTC)	3
13	AG ⁺ CCUGp	1994.29	996.14	Observed	Assigned	Leu(CAA), Leu(CAG), Leu(GAG), Leu(TAA), Leu(TAG)	5
14	UAG ⁺ CG	1689.25	843.62	Observed	Assigned	Gln(CTG), Gln(TTG)	2

Table S4B. List of RNA fragments with m¹A58 (RNase A-digestion)

No.	Sequence of RNA fragments	Molecular mass	<i>m/z</i> (-2)	Mass spectrum	CID	Possible tRNAs	# of tRNAs
1	Cmm ¹ Im ¹ AAUp	1659.27	828.63	Observed	Assigned	Ala(CGC), Ala(GGC), Arg(GCG), Arg(TCG), Asp(GTC), Cys(GCA), Glu(CTC), Glu(TTC), Gly(CCC), Gly(GCC), Gly(TCC), His(GTG), iMet(CAT), Leu(CAA), Leu(CAG), Leu(GAG), Leu(TAG), Phe(GAA), Pro(CGG), Pro(GGG), Pro(TGG), Ser(CGA), Ser(GCT), Ser(GGA), Ser(TGA), Thr(CGT), Thr(GGT), Thr(TGT), Trp(CCA), Tyr(GTA)	30
2	CmGm ¹ AAUp	1660.26	829.12	Observed	Assigned	Ala(TGC), Arg(CCG), Arg(TCT), Asn(GTT), Gln(CTG), Gln(TTG), Leu(TAA), Lys(CTT), Lys(TTT), Val(CAC), Val(GAC), Val(TAC)	12
3	Cmm ¹ Im ¹ AAGCp	2003.33	1000.66	Observed	Assigned	Ile(CAT), eMet(CAT)	2
4	CmGm ¹ AAGCp	2004.32	1001.15	Observed	Assigned	Arg(CCT), Ile(GAT)	2

Table S4C. List of RNA fragments with m²G10/m^{2,2}G10 or m^{2,2}G26 (RNase T₁-digestion)

No.	Sequence of RNA fragments	Molecular mass	<i>m/z</i> (-1 or -2)	Mass spectrum	CID	Possible tRNAs	# of tRNAs
1	Um ¹ Am ² Gp (position 10)	1008.16	1007.15	Observed	Assigned	Ala(CGC), Ala(GGC), Ala(UCG), Arg(CCT), Arg(TCT), Asn(GTT), Gly(CCC), Gly(GCC), Gly(TCC), Leu(CAG), Leu(TAG), Lys(CTT), Lys(TTT), Ile(CAT), eMet(CAT), Phe(GAA), Ser(CGA), Ser(GCT), Ser(GGA), Thr(CGT), Thr(TGT), Tyr(GTA)	22
2	m ^{2,2} GUGp (position 10)	1024.15	1023.14	Observed	Assigned	Asp(GTC), Gln(CTG), Gln(TTG), Glu(CTC), Glu(TTC), His(GTG), Trp(CCA)	7
3	Cm ^{2,2} GCCGp (position 26)	1633.25	815.62	Observed	Assigned	Ala(CGC), Ala(GGC), Arg(TCT), Asn(GTT), Phe(GAA), Ser(GCT)	6
4	Cm ^{2,2} GUCGp (position 26)	1634.23	816.11	Observed	Assigned	Ala(TGC), Arg(CCG), Arg(TCG)	3

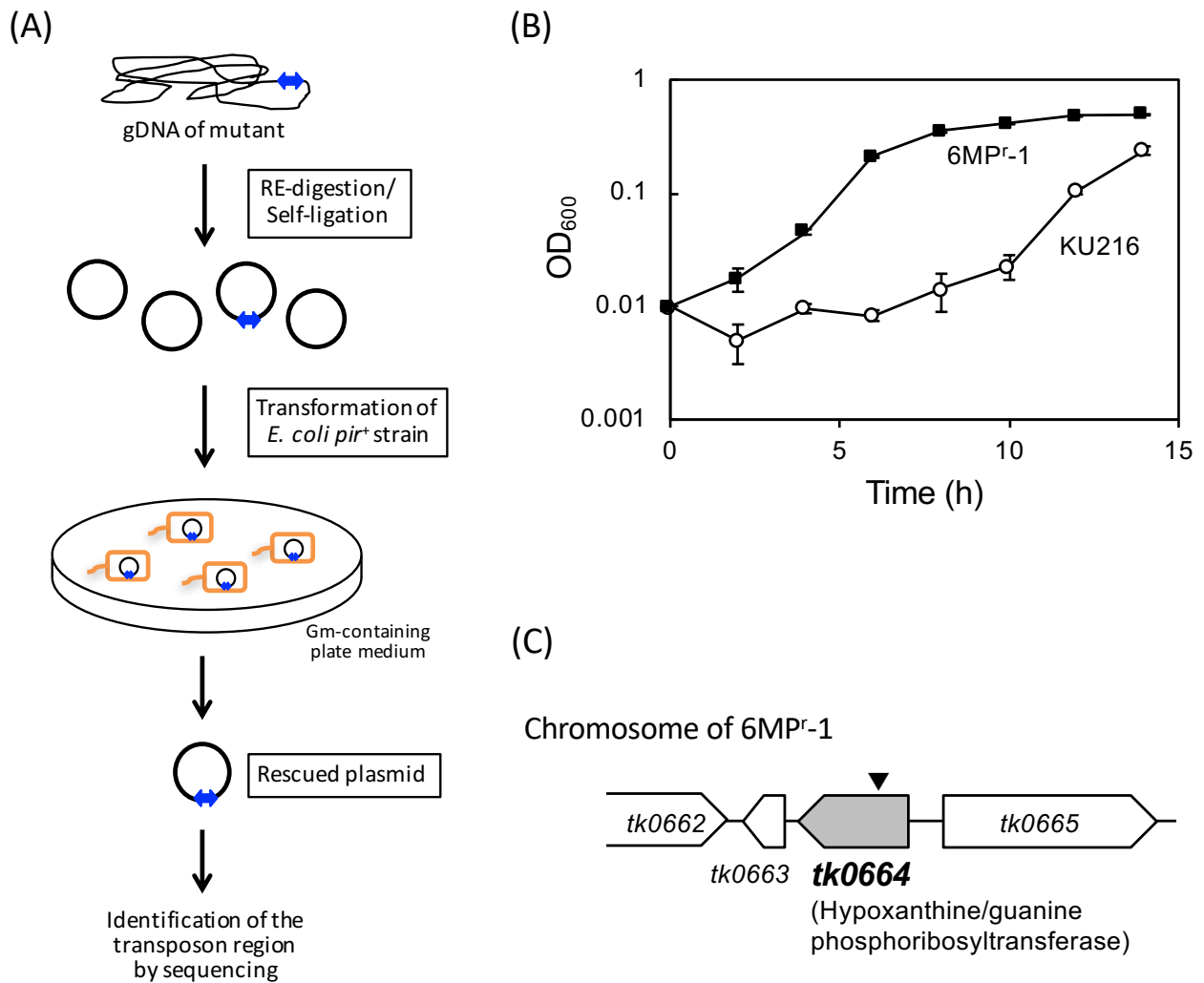


Fig. S1. (A) Scheme of plasmid rescue for identification of a transposon-inserted region in the isolated mutant. The blue double-headed arrow indicates the artificial transposon region containing R6Kg ori and gentamycin (Gm)-resistant cassette. (B) Growth of 6-methylpurine (6MP)-resistant mutant 6MP^r-1 (■) and control strain KU216 (○) of *T. kodakarensis* in ASW-YT-S⁰ medium containing 0.5 mM 6MP at 85°C. (C) Gene organization of the transposon-inserted region in *T. kodakarensis* 6MP^r-1 chromosome. The transposon region in 6MP^r-1 was identified within *tk0664* with direct repeat of 148-156 bp region of the gene.

[tRNA modification mutants]

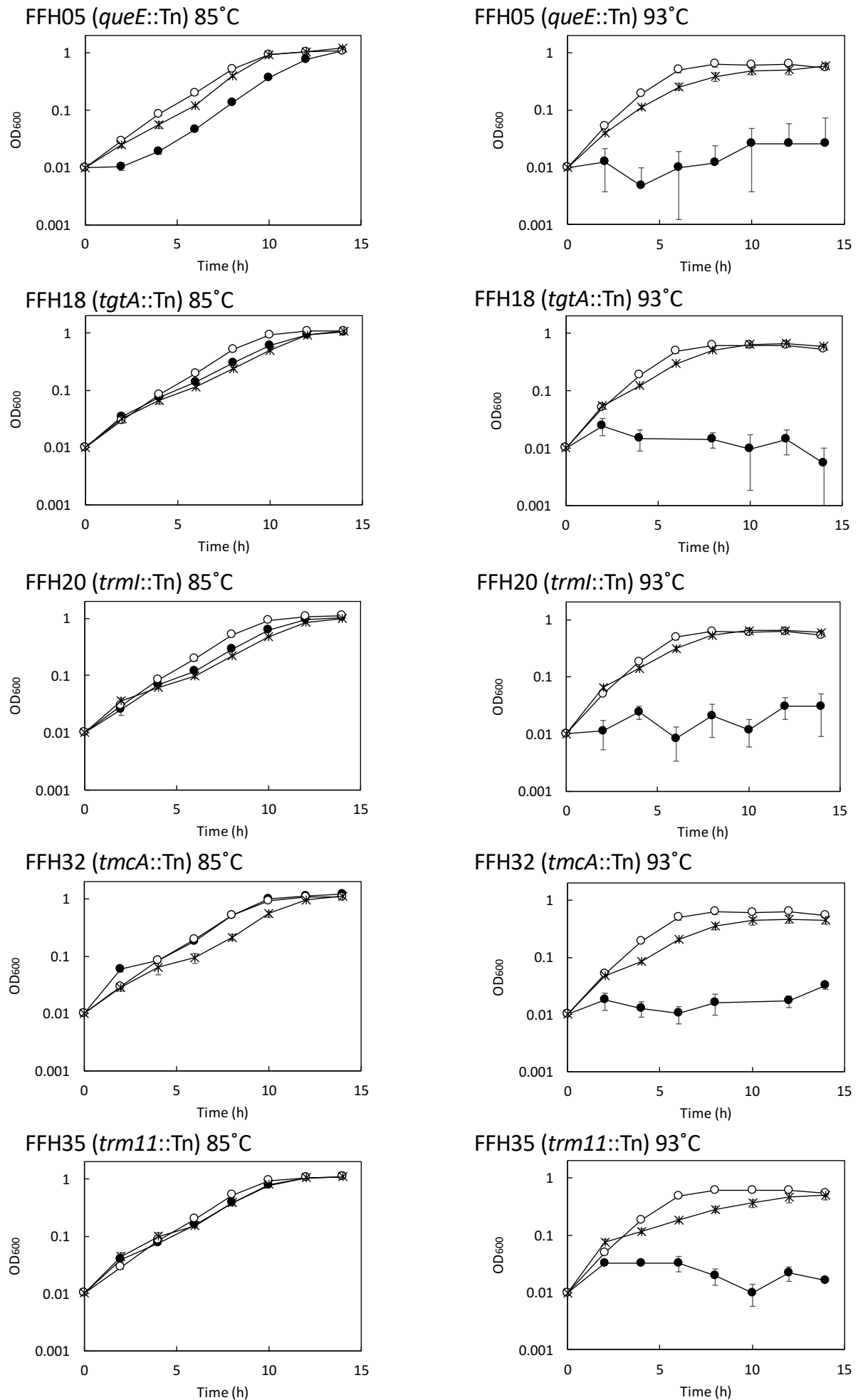


Fig. S2. Growth properties of *T. kodakarensis* tRNA modification mutants (●), their complemented strains (×), and control strain KD2239 (○) (n = 3).

[Other mutants]

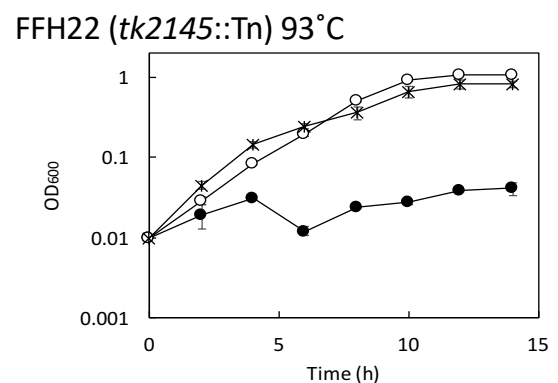
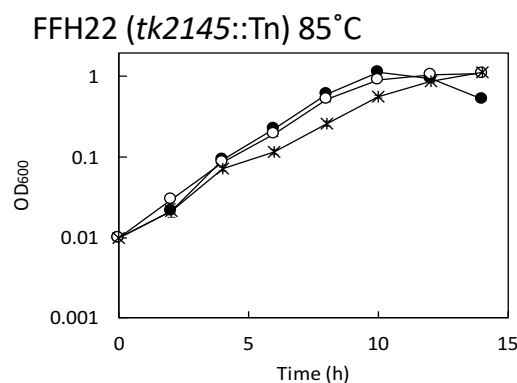
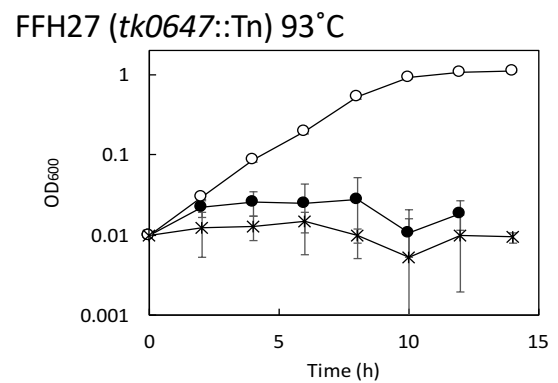
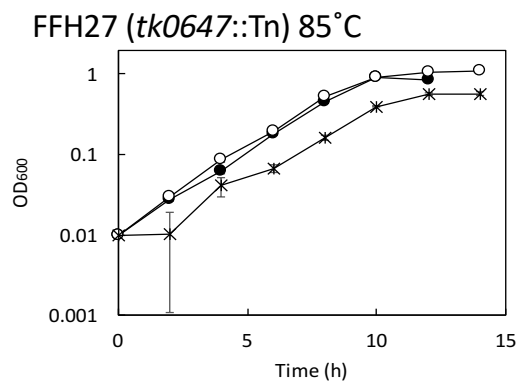
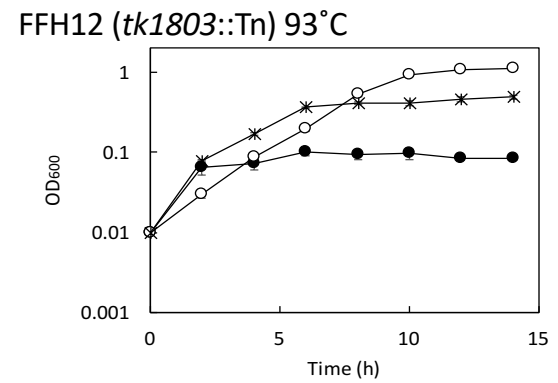
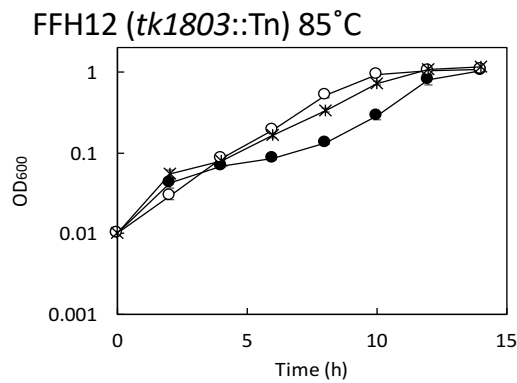
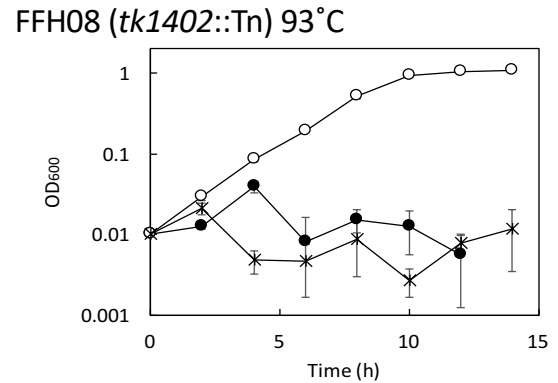
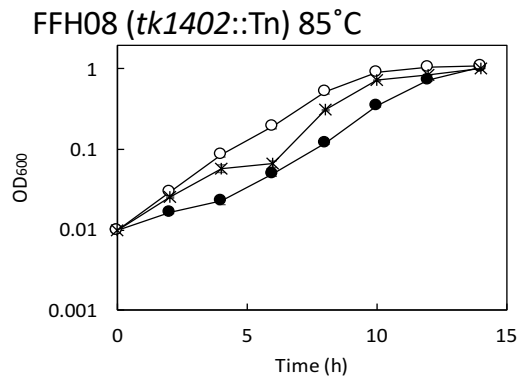
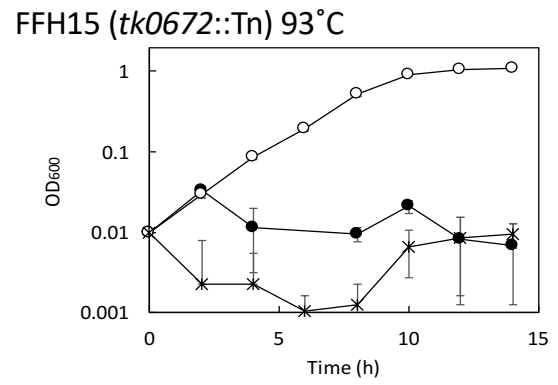
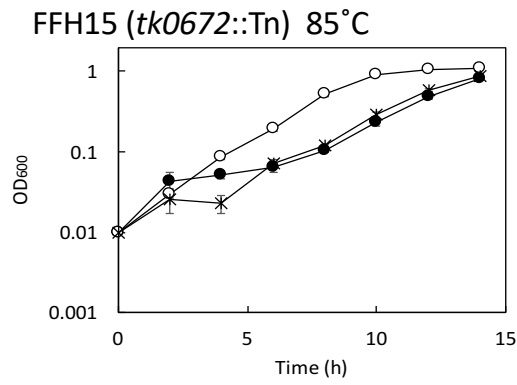


Fig. S3. Growth properties of *T. kodakarensis* thermosensitive mutants other than tRNA modification mutants (●), their complemented strains (×), and control strain KD2239 (○) (n = 3).

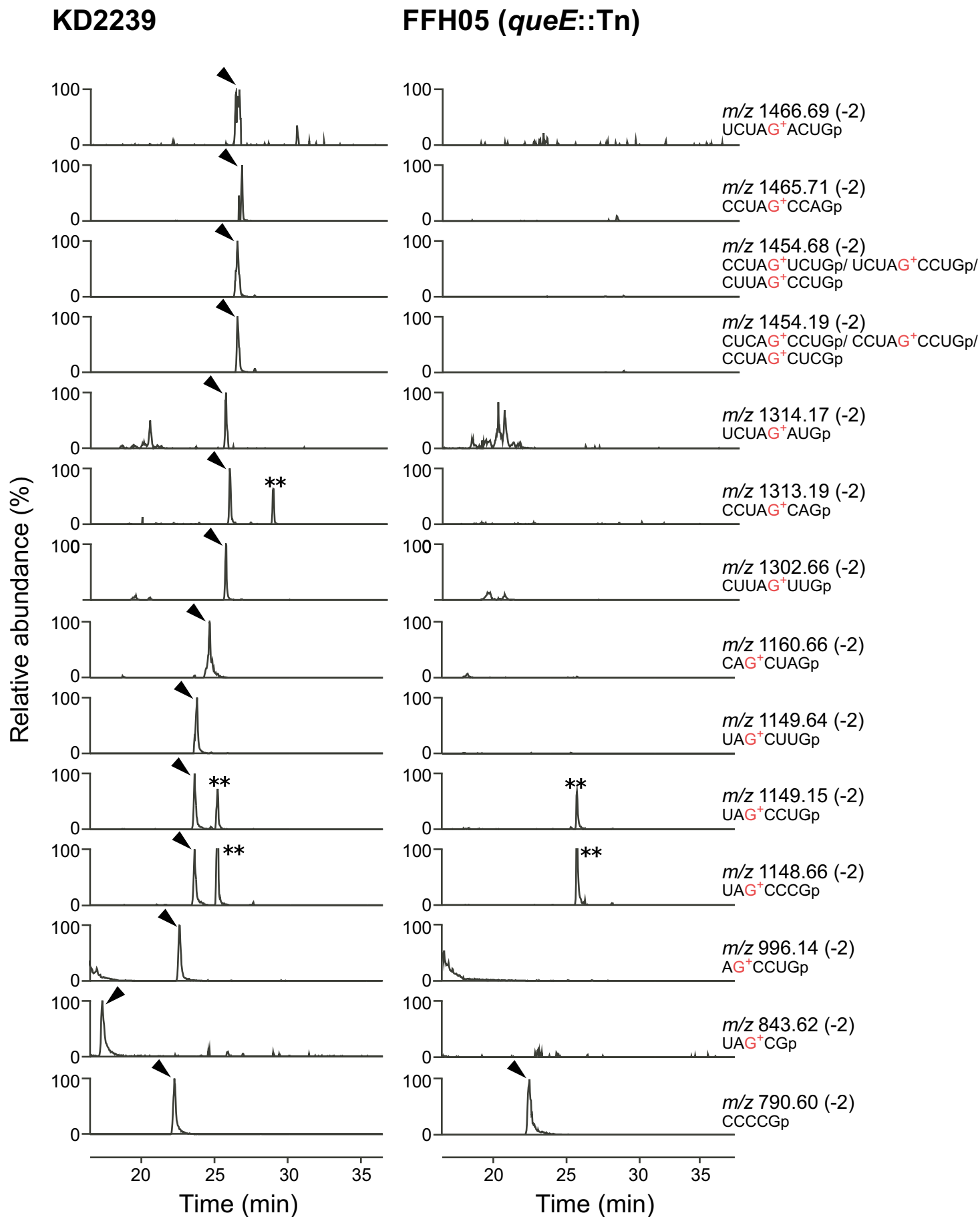


Fig. S4. Shotgun analysis of tRNA fragments generated by RNase T₁-digestion of tRNA extracted from *T. kodakarensis* KD2239 and FFH05 (*queE::Tn*). The panels represent the mass chromatograms that detect negatively charged ions of RNA fragment containing a nucleotide at position 15. The relative abundance represents relative intensity of each peak normalized by the intensity of CCCCg_p fragment. The peaks of the corresponding fragments are indicated by black arrowheads. Double asterisks indicate unassigned ions.

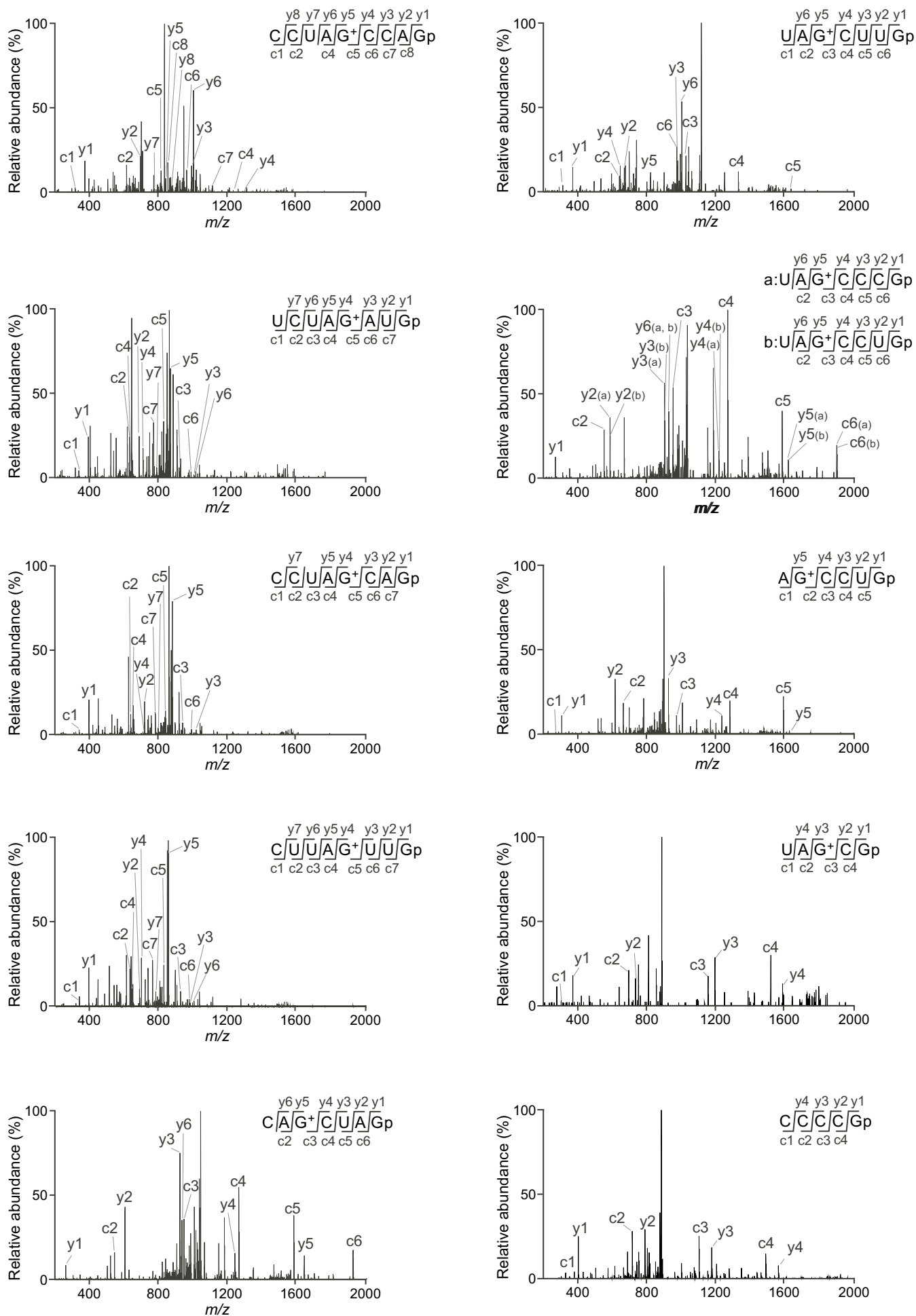


Fig. S5. CID spectra of ten RNA fragments having G⁺15 along with CCCCp fragment used as the internal standard in Fig. S4. Negatively charged ions of the individual fragments were used as precursor ions for CID analysis. The product ions in each the CID spectrum are assigned on the sequences.

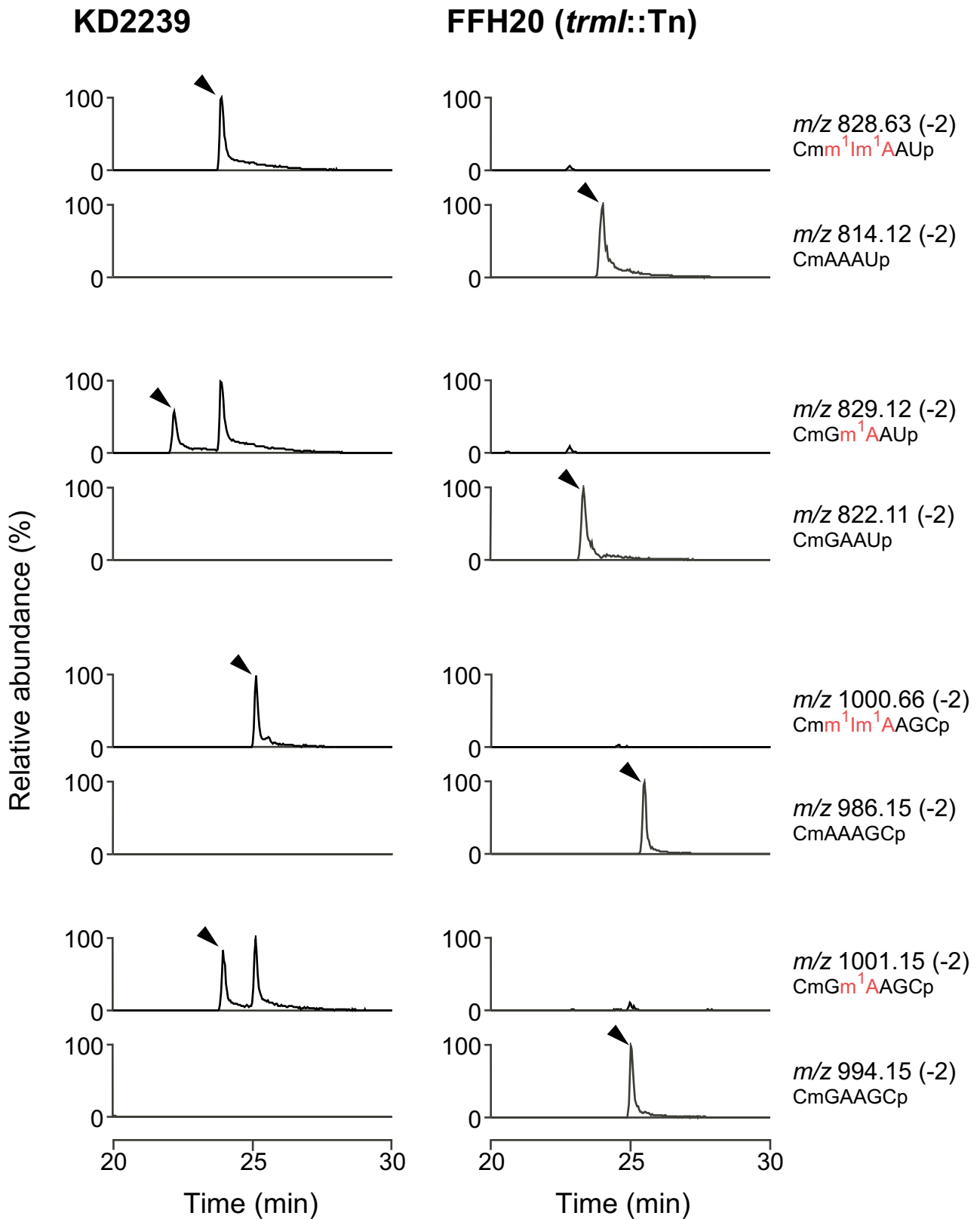


Fig. S6. Shotgun analysis of tRNA fragments generated by RNase A-digestion of tRNA extracted from *T. kodakarensis* KD2239 and FFH20 (*trmI::Tn*). The panels represent the mass chromatograms that detect divalent negatively charged ions of RNA fragment containing nucleotides from positions 56 to 60. The relative abundance represents relative intensity of each peak normalized by the highest peak. The peaks of the assigned fragments are indicated by black arrowheads

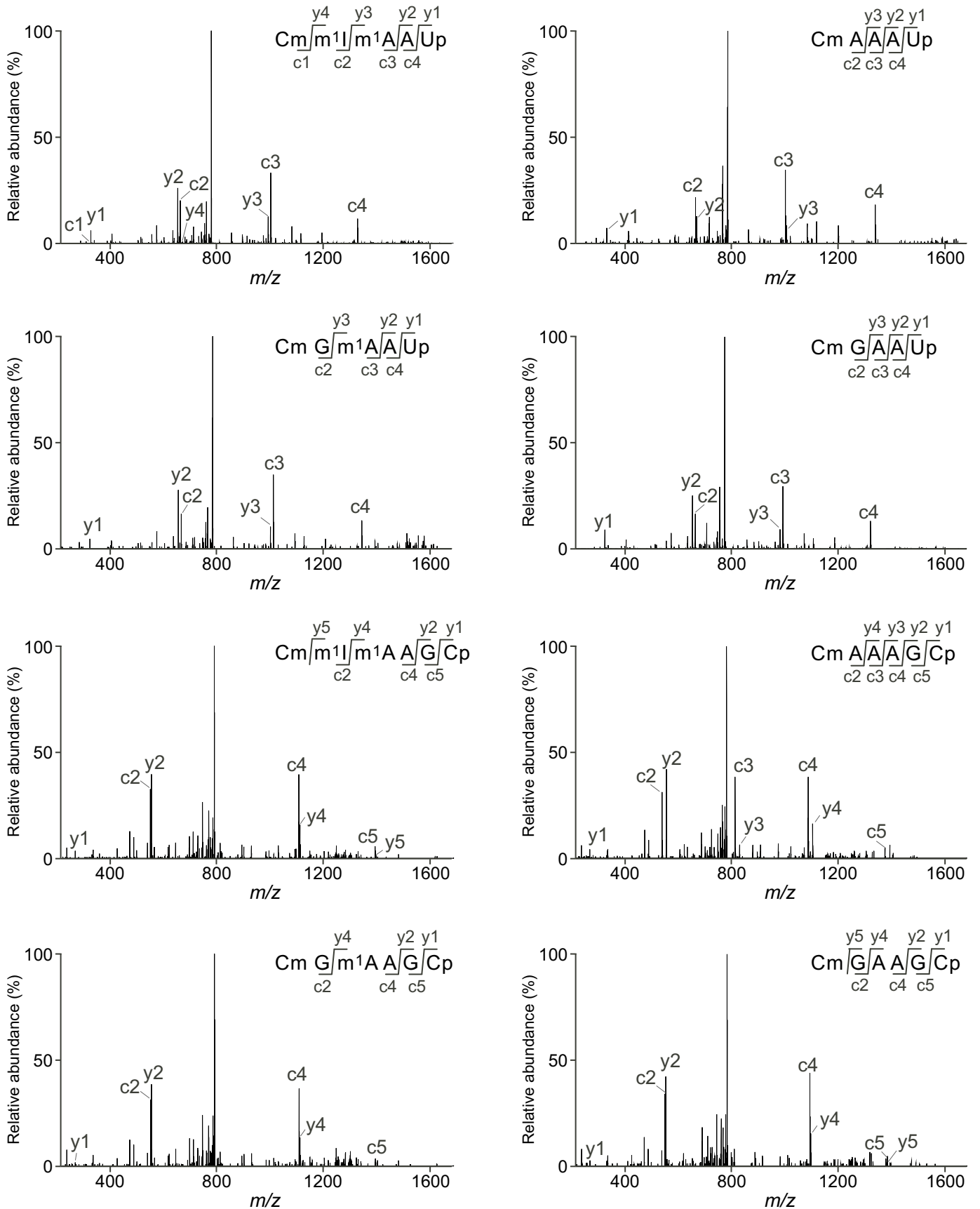


Fig. S7. CID spectra of eight RNase A digested-RNA fragments detected in Fig. S6. Negatively charged ions of the individual fragments were used as precursor ions for CID analysis. The product ions in each the CID spectra are assigned on the sequences.

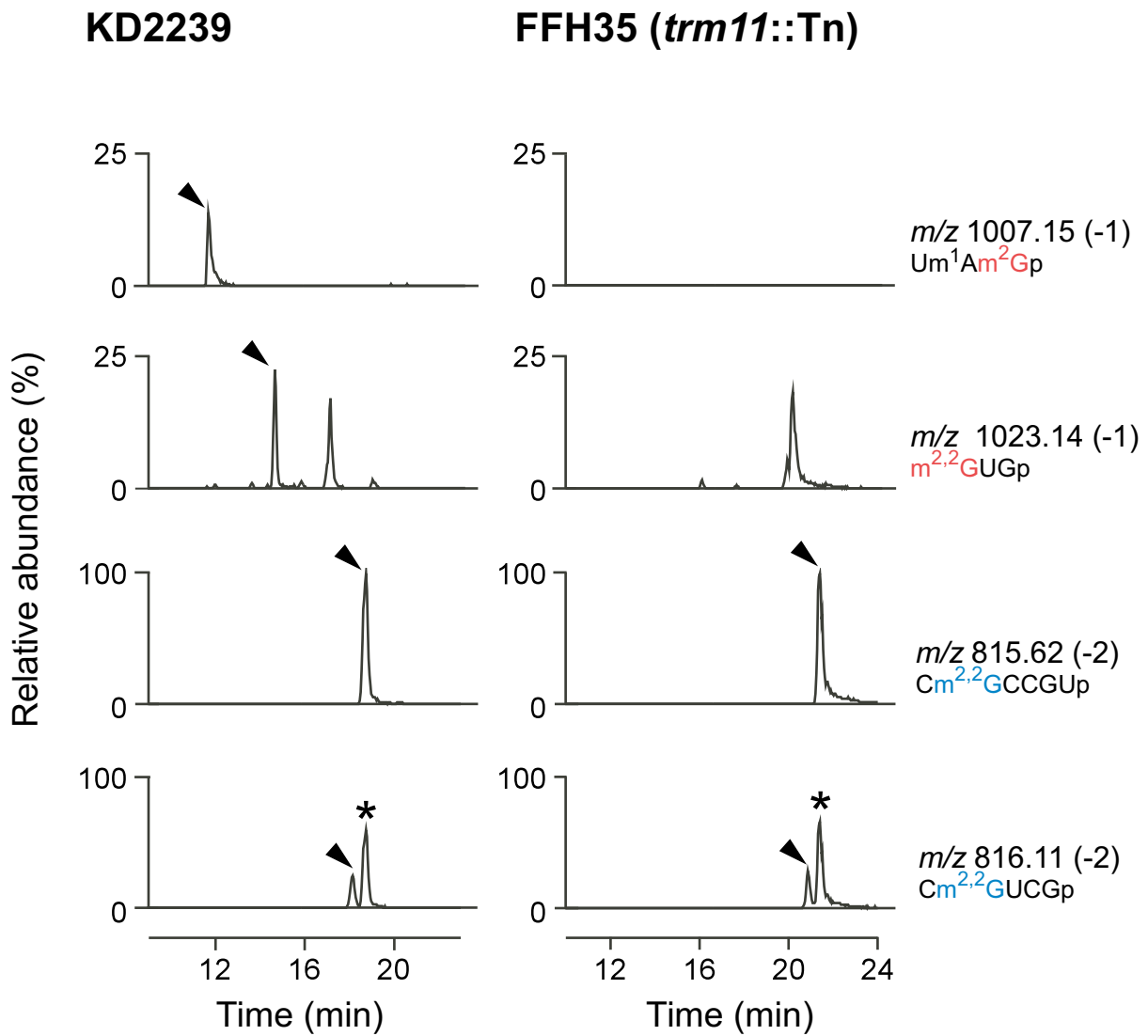


Fig. S8. Shotgun analysis of tRNA fragments generated by RNase T₁-digestion of tRNA extracted from *T. kodakarensis* KD2239 and FFH35 (*trm11::Tn*). The panels represent the mass chromatograms that detect monovalent or divalent negatively charged ions of RNA fragments containing the nucleotide at position 10 or 26. The relative abundance represents relative intensity of each peak normalized by intensities of Cm^{2,2}GCCGp fragments. The peaks of the assigned fragments are indicated by black arrowheads. Asterisks indicate peaks of Cm^{2,2}GCCGp fragments. Guanosines at positions 10 and 26 are shown in red and blue, respectively.

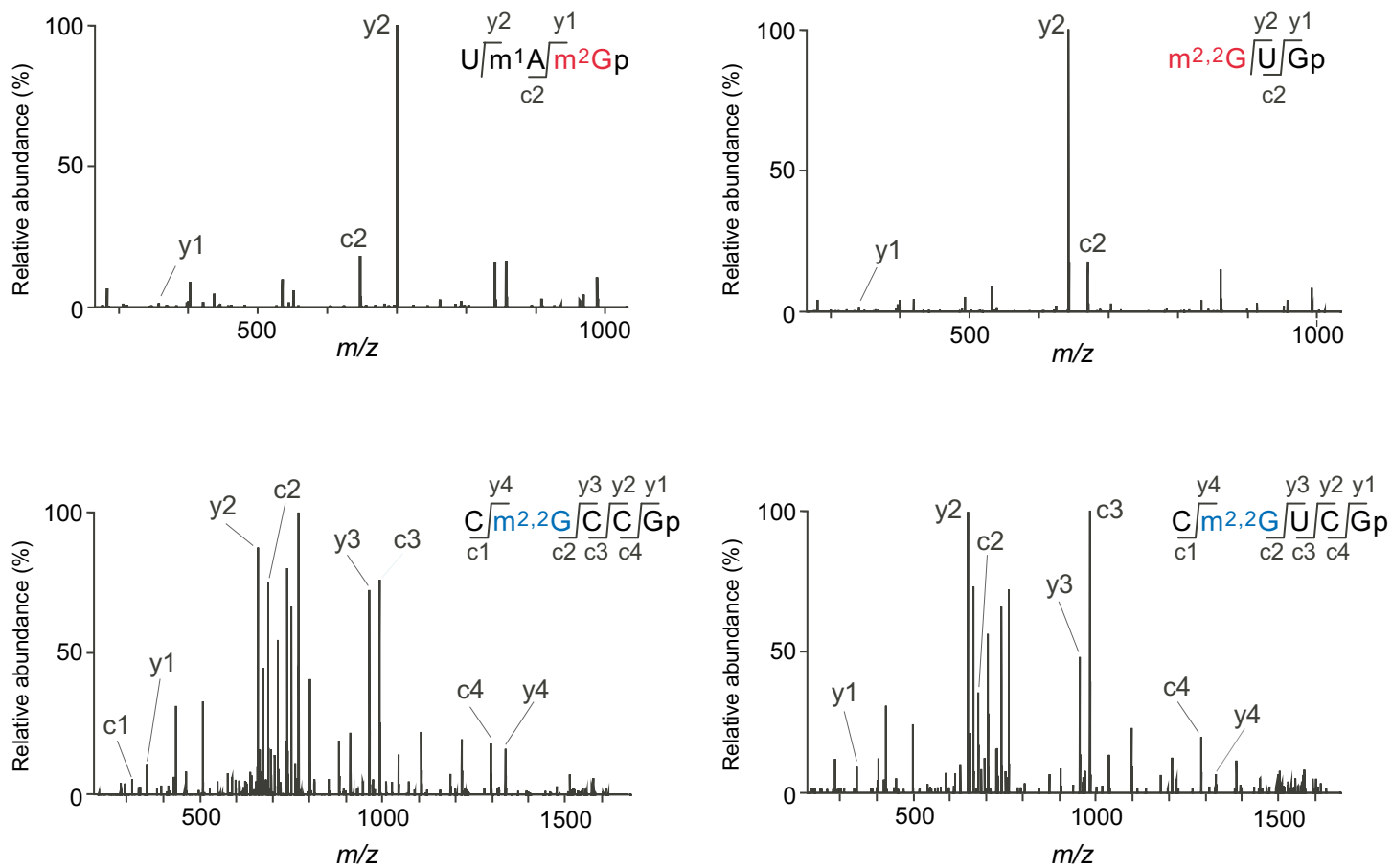


Fig. S9. CID spectra of four RNase T₁-digested tRNA fragments containing m²G/m^{2,2}G from *T. kodakarensis* KD2239 detected in Fig. S8. Monovalent or divalent negative ions were used as precursor ions for CID analysis. The product ions in each the CID spectra are assigned on the sequences. Guanosines at positions 10 and 26 are shown in red and blue, respectively.